J IRAN CHEM SOC
DOI 10.1007/s13738-013-0273-x

ORIGINAL PAPER

Unique charge-separated intermolecular and eight-membered intramolecular H-bonds in bis-(thio)barbiturates

Nader Noroozi Pesyan · Mohammad Jalilzadeh · Nasim Yalabi Torkaman · Ertan Şahin

Received: 2 February 2013 / Accepted: 9 May 2013

Abstract Reaction of symmetrical and unsymmetrical (thio)barbituric acids with aldehydes in the presence of triethylamine afforded a new form of bis-(thio)barbiturate containing charge-separated inter- and eight-membered intramolecular H-bonds. The reaction products were obtained as bis-(thio)barbiturates containing eight-membered intramolecular H-bond in the presence of L-(+)-tartaric acid (TA). The intramolecular H-bond strength (kcal/mol) and corresponding p*K*a value for **4ab′** were estimated to be 37 kcal/mol and −1.3, respectively.

Keywords Barbituric acid · Negative charge-assisted H-bonds · Resonance-assisted H-bonds · Eight-membered intramolecular H-bond · L-(+)-Tartaric acid

Electronic supplementary material The online version of this article (doi:10.1007/s13738-013-0273-x) contains supplementary material, which is available to authorized users.

N. N. Pesyan (✉)
Department of Chemistry, Faculty of Science, Urmia University, 57159 Urmia, Iran
e-mail: n.noroozi@urmia.ac.ir; nnp403@gmail.com

M. Jalilzadeh
Department of Chemistry, Faculty of Science, Islamic Azad University, Ahar Branch, Ahar, Iran

N. Y. Torkaman
Department of Chemistry, Faculty of Science, Tabriz Payam-e-noor University, Tabriz, Iran

E. Şahin
Department of Chemistry, Faculty of Science, Atatürk University, 25240 Erzurum, Turkey

Introduction

Hydrogen bond plays a key and major role in biological and pharmaceutical systems and remains a topic of intense current interest. This future judged enormous continuing amount of literature. Few selected recent articles exemplify the general scope of the topic, ranging from the role of H-bonding in weak interaction in gas phase [1, 2], supramolecular assemblies [3–6], helical structures [7], promoting catalytic enantioselective reactions [8–10] and molecular rotors [11] as well as through measurement of H-bond acidity of organic molecules [12]. Important consequences of both inter- and intramolecular H-bonding have long been recognized in the physicochemical behavior of DNA and RNA [13]. Another compound consisting of an eight-membered intramolecular H-bond has also been reported [14–22]. In the past decade, some quinoline and pyridine bis-barbiturates (Scheme 1) involving anticancer effect have been reported by Neumann et al. [23].

A search of the literature showed no report on the charge-separated intermolecular and eight-membered intramolecular H-bonds in (thio)barbiturates under basic and/or acidic conditions. Based on these concepts, herein, we report the charge-separated intermolecular and eight-membered intramolecular H-bonds in the reaction between (thio)barbituric acids with aldehydes in the presence of L-(+)-TA and/or triethylamine.

Experimental

General

The drawing and nomenclature of compounds were done by ChemBioDraw Ultra 12.0 version software. Melting

Published online: 05 June 2013

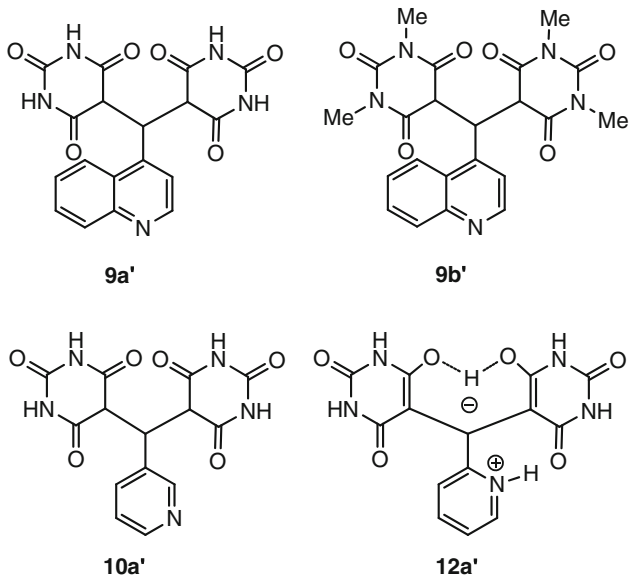

Scheme 1 Formula structure of some bis-barbiturate having anticancer properties [23, 25–27]

points were measured with an electrothermal digital apparatus and uncorrected. IR spectra were determined on a NEXUS 670 FT-IR spectrometer by preparing KBr pellets. The ^{1}H and ^{13}C NMR spectra were recorded on Bruker 300 FT-NMR at 300 and 75 MHz, respectively (Urmia University, Urmia, Iran). ^{1}H and ^{13}C NMR spectra were obtained on solution in DMSO-d_6 and/or in $CDCl_3$ as solvents using TMS as internal standard. The data are reported as (s = singlet, d = doublet, t = triplet, q = quartet, m = multiplet or unresolved, bs = broad singlet, coupling constant(s) in Hz, integration). All reactions were monitored by TLC with silica gel-coated plates (AcOEt:AcOH/80:20/v:v). The X-ray analysis of compound **4ab′** was used for data collection on a four-circle Rigaku R-AXIS RAPID-S diffractometer equipped with a two-dimensional area IP detector (Department of Chemistry, Atatürk University, Erzurum, Turkey). Compound **2e′** was synthesized in our laboratory based on reported literature [24]. Other starting materials and the solvents used were purchased from Merck without further purification. The physical and spectral data of the selected compounds are as follows.

General procedure for the preparation of **3ad′** as an example

In a 10 mL tube, equipped with a magnetic stirrer, with Teflon-faced screw cap, 0.19 g (0.96 mmol) 1,3-diethyl thiobarbituric acid and 0.07 g (0.48 mmol) 2-nitrobenzaldehyde were dissolved in 10 mL methanol and then 0.15 g (0.96 mmol) L-(+)-tartaric acid was added to the solution at 0 °C. The reaction mixture was stirred for 2 h at 0 °C to room temperature. The progression of reaction was monitored by thin layer chromatography (TLC). After a few minutes, a crystalline white solid precipitate was filtered off, washed with few milliliters of methanol and dried (0.18 g, 90 % yield).

*5,5′-((2-Nitrophenyl)methylene)bis(1,3-diethyl-6-hydroxy-2-thioxo-2,3-dihydropyrimidin-4(1H)-one) (**3ad′**)*

Colorless solid (80 %); mp = 212–214 °C. ^{1}H NMR ($CDCl_3$, 300 MHz) δ: 14.00 (bs, 1H, OH), 9.72, (bs, 1H, OH), 7.51–7.60 (m, 2H, CH–ar.), 7.42 (t, 1H, J = 7.5 Hz, CH–ar.), 7.28 (d, 1H, J = 7.5 Hz, CH–ar.), 6.11 (s, 1H, CH-aliph.), 4.52–4.68 (m, 8H, 4 N**CH$_2$**CH$_3$), 1.27-1.40 (m, 12H, 4 **CH$_3$**CH$_2$N); ^{13}C NMR ($CDCl_3$, 75 MHz) δ: 11.9, 32.6, 45.1, 45.4, 96.6, 124.1, 128.0, 129.5, 131.3, 132.7, 150.1, 162.0, 163.6, 164.4, 174.4; FT-IR (KBr, cm^{-1}) ν_{max}: 3438 (OH), 3050 (CH–ar.), 2981 (CH–aliph.), 2934 (CH–aliph.), 1691 (C=O), 1620 (C=C ar.), 1528 (NO2), 1487, 1380, 1264, 1110.

*5,5′-((4-Nitrophenyl)methylene)bis(1,3-diethyl-6-hydroxy-2-thioxo-2,3-dihydropyrimidin-4(1H)-one) (**3bd′**)*

Colorless solid (80 %), mp = 207–210 °C. ^{1}H NMR ($CDCl_3$, 300 MHz) δ: 14.0 (bs, 1H), 8.20 (d, 2H, J = 8.4 Hz, CH–ar.), 7.33 (d, 2H, J = 8.4 Hz, CH–ar.), 5.70 (s, 1H, CH-aliph.), 5.49 (bs, 1H, OH), 4.57–4.73 (m, 8H, 4 N**CH$_2$**CH$_3$), 1.39 (t, 6H, J = 6.9 Hz, 2 **CH$_3$**CH$_2$N), 1.30 (t, 6H, J = 6.9 Hz, 2 **CH$_3$**CH$_2$N); ^{13}C NMR ($CDCl_3$, 75 MHz) δ: 12.0, 35.3, 44.7, 45.3, 96.7, 123.7, 127.4, 143.7, 162.3, 163.8, 174.6; FT-IR (KBr, cm^{-1}) ν_{max}: 3433 (OH), 3040 (CH–ar.), 2985 (CH–aliph.), 2934, 2877 (CH–aliph.), 1621 (C=O), 1520 (NO2), 1430, 1380, 1348, 1264, 1107.

*5,5′-((3-Nitrophenyl)methylene)bis(1,3-diethyl-6-hydroxy-2-thioxo-2,3-dihydropyrimidin-4(1H)-one) (**3cd′**)*

Colorless solid (80 %), mp = 206–207 °C. ^{1}H NMR ($CDCl_3$, 300 MHz) δ: 14.00 (bs, 1H, OH), 8.43 (bs, 1H, OH), 7.20 (t, 1H, J = 7.8 Hz, CH–ar.), 6.70 (d, 2H, J = 4.8 Hz, CH–ar.), 6.64 (s, 1H, CH–ar.), 5.63 (s, 1H, CH-aliph.), 4.58–4.70 (m, 8H, 4 N**CH$_2$**CH$_3$), 1.38 (t, 6H, J = 6.9 Hz, 2 **CH$_3$**CH$_2$N), 1.30 (t, 6H, J = 6.9 Hz, 2 **CH$_3$**CH$_2$N); ^{13}C NMR ($CDCl_3$, 75 MHz) δ: 12.0, 12.1, 34.8, 44.6, 45.1, 97.3, 113.6, 113.7, 118.7, 129.6, 137.7, 155.8, 162.2, 163.7, 174.5; FT-IR (KBr, cm^{-1}) ν_{max}: 3435 (OH), 3030 (CH–ar.), 2982 (CH–aliph.), 2932 (CH–aliph.), 1620 (C=O), 1528 (NO_2), 1434, 1380, 1266, 1109.

*5,5′-((3-Hydroxyphenyl)methylene)bis(1,3-diethyl-6-hydroxy-2-thioxo-2,3-dihydropyrimidin-4(1H)-one) (**3dd′**)*

Colorless solid (70 %), mp = 244 °C. ^{1}H NMR ($CDCl_3$, 300 MHz) δ: 14.00 (bs, 1H, OH), 8.06 (bs, 2H, 2 OH), 7.19 (t, 1H, J = 7.8 Hz, CH–ar.), 6.71 (d, 2H, J = 7.5 Hz, CH–ar.), 6.64 (s, 1H, CH–ar.), 5.63 (s, 1H, CH-aliph.), 4.58–4.70 (m, 8H, 4 N**CH$_2$**CH$_3$), 1.38 (t, 6H, J = 6.9 Hz, 2 **CH$_3$**CH$_2$N), 1.30 (t, 6H, J = 6.9 Hz, 2 **CH$_3$**CH$_2$N); ^{13}C NMR ($CDCl_3$, 75 MHz) δ: 12.0, 12.1, 34.8, 44.6, 45.1, 97.3, 113.5, 113.7, 118.8, 129.6, 137.7, 155.8, 162.2, 163.7, 174.6; FT-IR (KBr, cm^{-1}) ν_{max}: 3458 (OH), 3020 (CH–ar.), 2982 (CH–aliph.), 2932 (CH–aliph.), 1620 (C=O), 1432, 1377, 1265, 1109.

*5,5′-((3,4,5-Trimethoxyphenyl)methylene)bis(1,3-diethyl-6-hydroxy-2-thioxo-2,3-dihydropyrimidin-4(1H)-one) (**3ed′**)*

Colorless solid (70 %), mp = 155 °C. ^{1}H NMR ($CDCl_3$, 300 MHz) δ: 13.9 (bs, 1H, OH), 12.10 (bs, 1H, OH), 6.31 (s, 2H, CH–ar.), 5.62 (s, 1H, CH-aliph.), 4.50–4.70 (m, 8H, 4 N**CH$_2$**CH$_3$), 3.84 (s, 3H, OCH$_3$), 3.76 (s, 6H, 2 OCH$_3$), 1.37 (t, 6H, J = 6.9 Hz, 2 **CH$_3$**CH$_2$N), 1.30 (t, 6H, J = 6.9 Hz, 2 **CH$_3$**CH$_2$N); ^{13}C NMR ($CDCl_3$, 75 MHz) δ: 12.0, 12.1, 34.9, 44.5, 45.2, 56.4, 60.9, 97.5, 104.1, 131.1, 137.1, 153.2, 162.2, 163.7, 174.6; FT-IR (KBr, cm^{-1}) ν_{max}: 3436 (OH), 2977 (CH–aliph.), 2934 (CH–aliph.), 1619 (C=O), 1427, 1381, 1267, 1108.

*5,5′-((4-Fluorophenyl)methylene)bis(1,3-diethyl-6-hydroxy-2-thioxo-2,3-dihydropyrimidin-4(1H)-one) (**3fd′**)*

Colorless solid (70 %), mp = 189–190 °C. ^{1}H NMR ($CDCl_3$, 300 MHz) δ: 13.90 (bs, 1H, OH), 6.99–7.10 (m, 5H), 5.63 (s, 1H, CH-aliph.), 4.57–4.73 (m, 8H, 4 N**CH$_2$**CH$_3$), 1.38 (t, 6H, J = 6.9 Hz, 2 **CH$_3$**CH$_2$N), 1.30 (t, 6H, J = 6.9 Hz, 2 **CH$_3$**CH$_2$N); ^{13}C NMR ($CDCl_3$, 75 MHz) δ: 11.99, 12.05, 34.4, 44.6, 45.2, 97.4, 115.2, 115.5, 127.9, 128.0, 131.1, 162.2, 163.2, 163.7, 174.6; FT-IR (KBr, cm^{-1}) ν_{max}: 3432 (OH), 2975, 2918, 2849 (CH–aliph.), 1620 (C=O), 1438, 1383, 1267, 1111.

*5,5′-(Phenylmethylene)bis(1,3-diethyl-6-hydroxy-2-thioxo-2,3-dihydropyrimidin-4(1H)-one) (**3gd′**)*

Colorless solid (70 %), mp = 188–190 °C. ^{1}H NMR ($CDCl_3$, 300 MHz) δ: 13.90 (bs, 1H), 7.29–7.36 (m, 3H, CH–ar.), 7.14 (d, 2H, J = 7.2 Hz, CH–ar.), 6.76 (bs, 1H, OH), 5.68 (s, 1H, CH-aliph.), 4.58–4.74 (m, 8H, 4 N**CH$_2$**CH$_3$), 1.39 (t, 6H, J = 6.9 Hz, 2 **CH$_3$**CH$_2$N), 1.31 (t, 6H, J = 6.9 Hz, 2 **CH$_3$**CH$_2$N); ^{13}C NMR ($CDCl_3$, 75 MHz) δ: 11.98, 12.06, 34.9, 44.6, 45.1, 97.4, 126.3, 126.8, 128.5, 135.0, 162.0, 163.0, 174.6; FT-IR (KBr, cm^{-1}) ν_{max}: 3444 (OH), 3028 (CH–ar.), 2978, 2933, 2873 (CH–aliph.), 1615 (C=O), 1436, 1383, 1267, 1110.

*Triethylammonium 5-((6-hydroxy-1,3-dimethyl-2,4-dioxo-1,2,3,4-tetrahydropyrimidin-5-yl)(2-nitrophenyl) methyl)-1,3-dimethyl-2,6-dioxo-1,2,3,6-tetrahydropyrimidin-4-olate (**4ab′**)*

In a 10 mL tube, equipped with a magnetic stirrer, with Teflon-faced screw cap, 0.15 g (0.96 mmol) 1,3-dimethyl barbituric acid and 0.07 g (0.48 mmol) 2-nitrobenzaldehyde were dissolved in 10 mL methanol and then 0.1 g (0.14 mL) triethylamine was added to the solution at 0 °C. The reaction mixture was stirred for 2 h at 0 °C to room temperature. The progression of reaction was monitored by thin layer chromatography (TLC). After a few minutes, a crystalline white solid precipitate was filtered off, washed with few milliliters of methanol and dried (0.17 g, 90 % yield). Colorless solid, mp = 308 °C (decomps.). ^{1}H NMR ($CDCl_3$, 300 MHz) δ: 16.2 (bs, 1H, OH), 9.62 (bs, 1H, NH), 7.24–7.44 (m, 4H, (CH–ar.)), 6.40 (s, 1H, CH-aliph.), 3.36–3.51 (m, 6H, 3 –CH$_2$–), 3.27 (s, 12H, 4 NCH$_3$), 1.33 (t, 9H, J = 6.9 Hz, 3 **CH$_3$**CH$_2$); ^{13}C NMR ($CDCl_3$, 75 MHz) δ: 8.7, 28.4, 32.0, 46.3, 50.6, 91.2, 123.7, 126.5, 129.9, 131.2, 136.1, 149.9, 151.9, 156.4, 163.8; FT-IR (KBr, cm^{-1}) ν_{max}: 3474 (OH), 3097 (CH–ar.), 2984 (CH–aliph.), 2947 (CH–aliph.), 1688 (C=O), 1615 (C=C ar.), 1526 (NO2).

*Triethylammonium 5-((1,3-diethyl-6-hydroxy-4-oxo-2-thioxo-1,2,3,4-tetrahydropyrimidin-5-yl) (2-nitrophenyl)methyl)-1,3-diethyl-6-oxo-2-thioxo-1,2,3,6-tetrahydropyrimidin-4-olate (**4ad′**)*

Yellow solid (80 %), mp = 210 °C (decomps.). ^{1}H NMR ($CDCl_3$, 300 MHz) δ: 9.70 (bs, 1H, OH), 7.30–7.50 (m, 4H, CH–ar.), 6.42 (s, 1H, CH-aliph.), 4.37–4.59 (m, 8H, 4 N**CH$_2$**CH$_3$), 3.39–3.43 (m, 6H, 3 –CH$_2$–), 2.30 (bs, 1H), 1.38 (t, 12H, J = 7.2 Hz, 4 **CH$_3$**CH$_2$N), 1.29 (t, 9H, J = 6.9 Hz, 3 CH$_3$CH$_2$); ^{13}C NMR ($CDCl_3$, 75 MHz) δ: 8.7, 12.2, 12.4, 32.2, 43.7, 44.1, 46.3, 96.1, 121.0, 123.9, 126.8, 129.7, 131.3, 150.1, 162.3, 162.6, 175.0; FT-IR (KBr, cm^{-1}) ν_{max}: 3438 (OH, NH), 3083 (CH–ar.), 2979 (CH–aliph.), 2932 (CH–aliph.), 2871 (CH–aliph.), 1640 (C=O), 1614, 1526, 1434, 1380, 1267, 1103, 781.

*Triethylammonium 5-((6-hydroxy-1-methyl-2,4-dioxo-1,2,3,4-tetrahydropyrimidin-5-yl)(2-nitrophenyl)methyl)-1-methyl-2,6-dioxo-1,2,3,6-tetrahydropyrimidin-4-olate (**4ae′**)*

Yellow solid (70 %), mp = 318 °C (decomps). ^{1}H NMR (DMSO-d_6, 300 MHz) δ: 16.25 (bs, 1H, OH), 10.28 (s, 2H, NH-BA), 8.75 (bs, 1H, NH-triethylammonium), 7.23–7.42

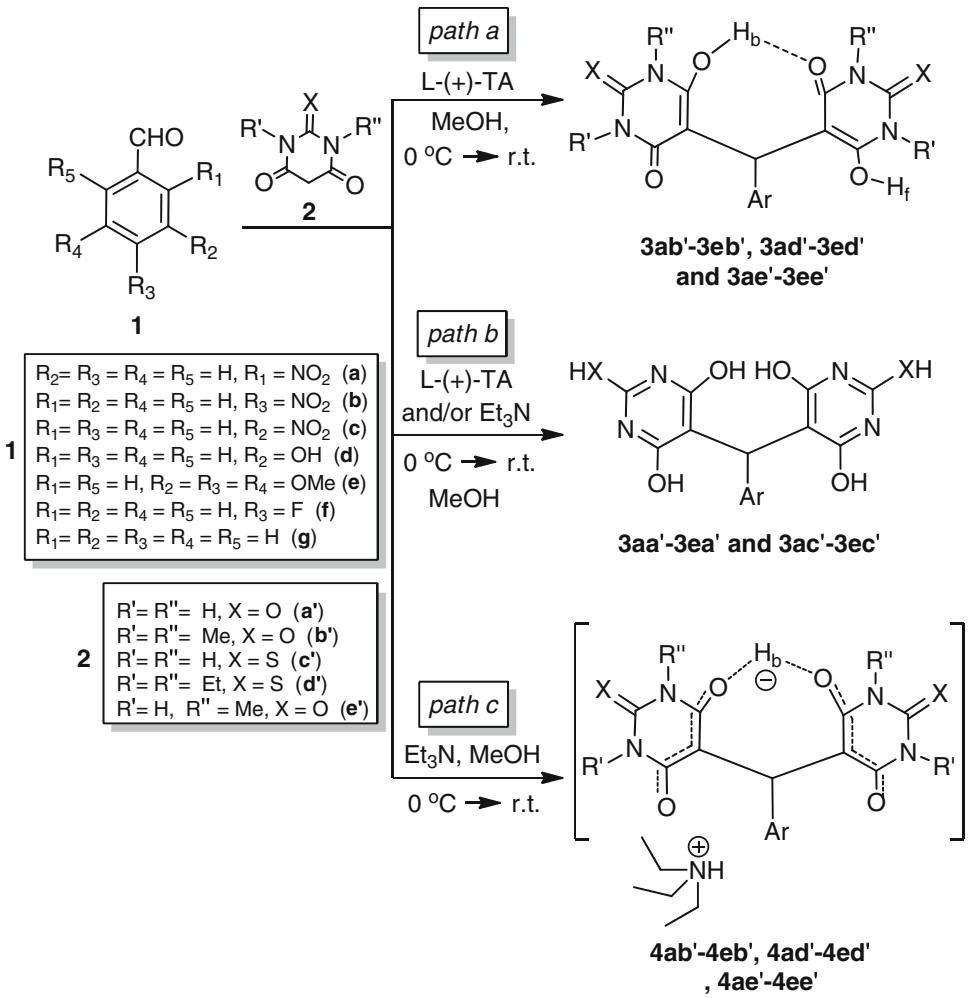

Scheme 2 Reaction of aldehydes with (thio)barbituric acids in the presence of L-(+)-TA (*path a*) and/or triethylamine (*paths b* and *c*)

(m, 4H, CH–ar.), 6.18 (s, 1H, CH-aliph.), 3.09 (q, 6H, $J = 7.2$ Hz, 3 –$\mathbf{CH_2}CH_3$), 3.03 (s, 6H, 2 NCH_3), 1.15 (t, 9H, $J = 7.2$ Hz, 3 $\mathbf{CH_3}CH_2$); ^{13}C NMR (DMSO-d_6, 75 MHz) δ: 9.1, 27.2, 30.9, 46.2, 90.4, 123.6, 126.5, 130.0, 131.1, 138.0, 150.3, 151.4, 162.6, 164.4; FT-IR (KBr, cm^{-1}) ν_{max}: 3450 (OH), 3068 (CH–ar.), 2993 (CH–aliph.), 1690 (C=O), 1610, 1527, 1461, 1363.

Results and discussion

This paper describes the formation of charge-separated intermolecular and eight-membered intramolecular H-bonds in the reaction of (thio)barbituric acids with aldehydes in the presence of triethylamine and/or L-(+)-TA to afford a new class of stable heterocyclic bis-(thio)barbiturates 5,5′-(arylmethylene)bis(6-hydroxy-1,3-dimethyl-pyrimidine-2,4(1*H*,3*H*)-diones) and their sulfur analogs 5,5′-(arylmethylene)bis(1,3-diethyl-6-hydroxy-2-thioxo-2,3-dihydropyrimidin-4(1*H*)-ones) (**3aa′–3ae′ through 3ga′–3ge′**) (Scheme 2).

The reaction between 3-nitrobenzaldehyde (**1c**) and 1,3-diethyl thiobarbituric acid (DETBA, **2d′**) were afforded Knoevenagel condensation then subsequently Michael adducts as; 5,5′-((2-nitrophenyl)methylene)bis(1,3-diethyl-6-hydroxy-2-thioxo-2,3-dihydropyrimidin-4(1*H*)-one) (**3cd′**) in the presence of L-(+)-TA (Scheme 2, path a). The structure of **3cd′** was confirmed by spectroscopic data. The ^{1}H NMR spectrum of this compound (in $CDCl_3$) revealed the presence of two different chemical shifts for *N*-ethyl protons as two distinct triplets at δ 1.30 and 1.38 ppm for methyl groups and a multiplet for two N–CH_2– groups at δ 4.58–4.69 ppm, respectively. A singlet for aliphatic C1–H proton at δ 5.63 ppm and two broad singlets at δ 8.43 and 14.00 ppm that corresponded to two types of exchangeable protons (the exchangeability was examined by adding a drop of D_2O) were found. A singlet at δ 6.64 (1H), a doublet at δ 6.71 (2H) and a triplet at δ 7.18 ppm (1H) at the aromatic region were observed. The ^{13}C NMR spectrum of **3 cd′** showed 15 distinct peaks that confirmed the structure of this compound (see "Experimental"; supplementary data).

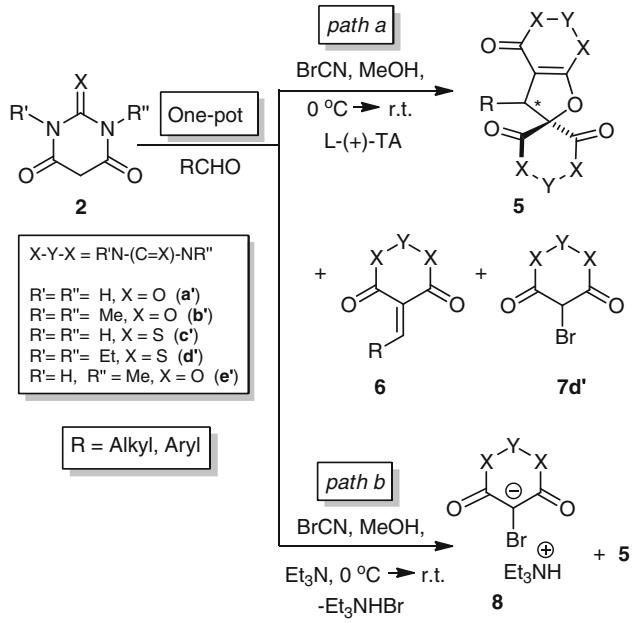

Scheme 3 Reaction of (thio)barbituric acids (**2a′–e′**) with cyanogen bromide and aldehydes in the presence of L-(+)-TA (*path a*) and comparison with their reaction in the presence of triethylamine (*path b*) [29–32]

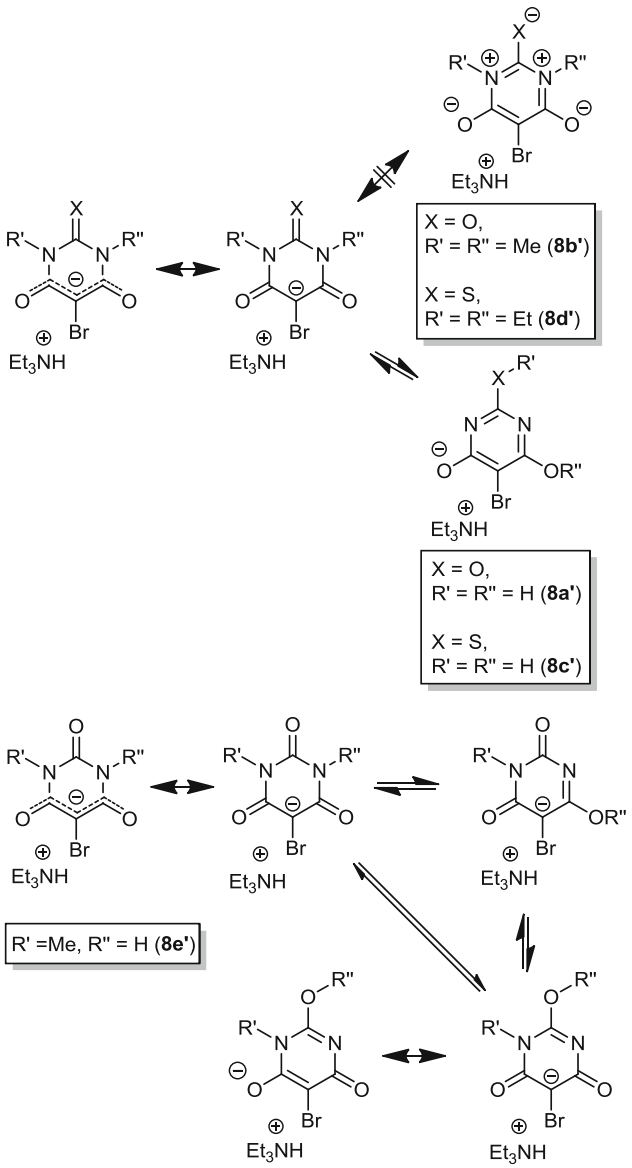

Scheme 4 Tautomeric and mesomeric forms of **8a′–8e′**

The Michael adducts derived from *N*,*N*′-dialkylated (thio)barbituric acids (**2b′** and **2d′**) and *N*-alkylated barbituric acid (**2e′**) exclusively showed an eight-membered intramolecular H-bond between the carbonyl group of one (thio)barbituric acid ring moiety and hydroxyl group of the enolic form of another (thio)barbituric acid ring moiety species (this proton is denoted by H_b) (Scheme 2, path a). Any of these types of barbiturates include amidic (–CO–NH–) and/or thioamidic protons (–CS–NH–) and do not show an eight-membered intramolecular H-bond. It seems that this phenomenon arose from tautomerization of (thio)barbituric acids (lactam–thiolactam $\rightleftharpoons$ lactim–thiolactim and/or lactam $\rightleftharpoons$ lactim forms) that occurred prior to formation of intramolecular H-bond (Scheme 2, path b). Therefore, among these compounds, **2b′**, **2d′** and **2e′** only show this type of intramolecular H-bonding.

As mentioned above, the electron-withdrawing substituents on the phenyl ring in 5-arylmethylene (thio)barbituric acids (as an α,β-unsaturated carbonyl compounds) facilitate the Michael addition on their β-position [28].

More recently, the reaction of various aldehydes [29–32] and ketones [33, 34] with (thio)barbituric acids and cyanogen bromide have been investigated in the presence of triethylamine and L-(+)-TA (Scheme 3). In these reactions, 5-aryl-1*H*,1′*H*-spiro[furo[2,3-*d*]pyrimidine-6,5′-pyrimidine] 2,2′,4,4′,6′(3*H*,3′*H*,5*H*)-pentaone (**5a′**), 5-aryl-1,1′,3,3′-tetramethyl-1*H*,1′*H*-spiro[furo[2,3-*d*]pyrimidine-6,5′-pyrimidine] 2,2′,4,4′,6′(3*H*,3′*H*,5*H*)-pentaone (**5b′**), 5-aryl-2,2′-dithioxo-2,2′,3,3′-tetrahydro-1*H*,1′*H*-spiro[furo[2,3-*d*] pyrimidine-6,5′-pyrimidine]-4,4′,6′(5*H*)-triones (**5c′**) and diastereomeric mixtures of 1′,3-dimethyl-5-aryl-1*H*,1′*H*-spiro[furo [2,3-*d*]pyrimidine-6,5′-pyrimidine]-2,2′,4,4′,6′(3*H*,3′*H*,5*H*)-pentaone (**5e′**) were obtained, respectively (Scheme 3) [29–32]. Elinson et al. [35] also reported the synthesis of spiro compounds **5** in the presence of bromine in alkali condition (EtONa/EtOH). No spiro compounds **5** were obtained in the absence of cyanogen bromide under the same condition. Exceptionally, the reaction of 1,3-diethyl thiobarbituric acid (**2d′**) with aldehydes (**1**) in the presence of cyanogen bromide produced **3d′** under the same condition. No spiro compounds **5d′** were obtained. The reason for the formation

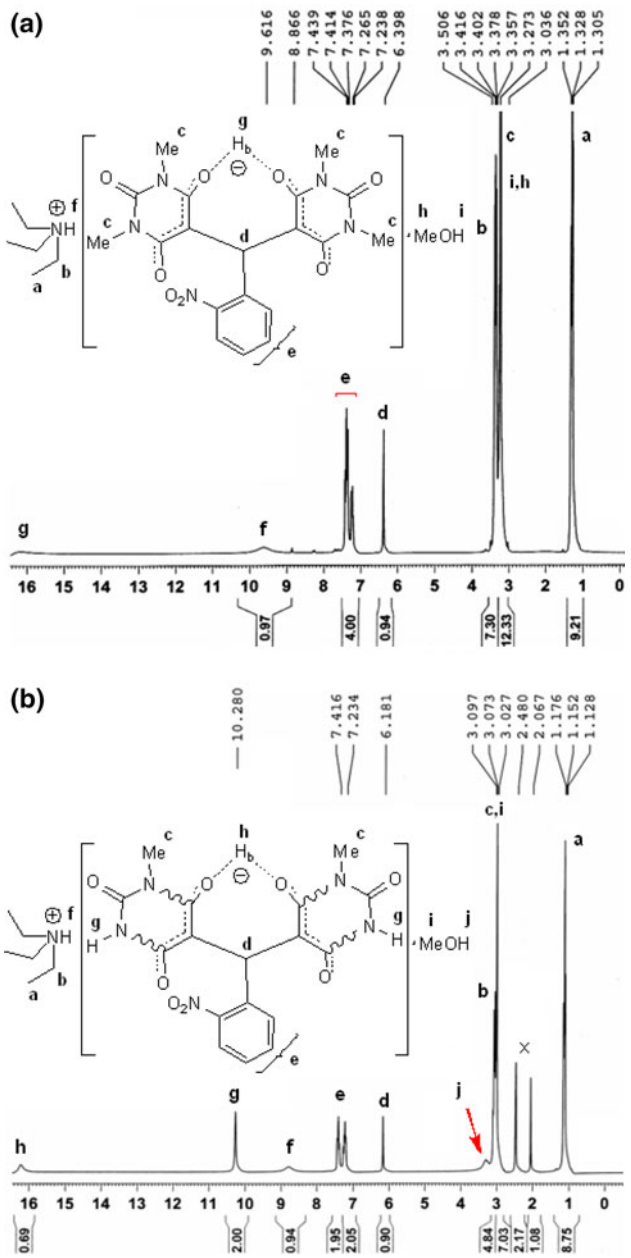

Fig. 1 ^{1}H NMR spectrum of **4ab′** (**a**) and **4ae′** (**b**)

of **3d′** in competition with the formation of **5d′** attributed to the strong nucleophilicity of 1,3-diethyl thiobarbituric acid **2d′** (Scheme 4) [30]. The nucleophilicity of **2d′** was stronger than that of 5-bromo-1,3-diethyl-6-hydroxy-2-thioxo-2,3-dihydropyrimidin-4(1*H*)-one (**7d′**). Therefore, **2d′** attacked the β-carbon position of **6cd′** as Michael addition prior to formation of **7d′**. In contrast, we detected **7d′** in the reaction of **2d′** with BrCN in the absence of aldehyde and in the presence of L-(+)-TA [30]. The ^{1}H NMR spectrum of **7d′** consists of a triplet at δ 1.32 and a quartet at δ 4.57 ppm corresponding to methyl and methylene protons on ethyl groups, respectively. A singlet at δ 10.15 ppm corresponds to the OH group of the predominant thiolactam-enol form. The ^{13}C NMR spectrum of **7d′** shows five distinct peaks at δ 175.4, 164.4, 90.3, 45.4 and 11.9 ppm that confirm the structure [30]. Other evidences for the formation of **7d′** (the existence of bromine atom in this molecule) were obtained by the Beilstein test and the wet silver nitrate test (precipitate of pale yellow silver bromide) [36].

As mentioned above, the reaction of aldehydes with (thio)barbituric acids in the presence of triethylamine afforded the salts of **4** (Scheme 2, path c). One of the most interesting phenomena in this research is the binding of triethylammonium salt moiety to some bis-barbiturates anion derived from **2b′**, **2d′** and **2e′** by intermolecular H-bonding in the ratio of 1:1. The crystallographic data and ^{1}H NMR spectra confirm the binding of triethylammonium cation moiety to the anionic form. This phenomenon is shown for **4ab′** and **4ae′** in Fig. 1, as examples. In **4ab′**, a triplet at δ 1.33 and a quartet at δ 3.41 ppm correspond to methyl and methylene protons on the ethyl groups of triethylammonium salt moiety, a singlet at δ 3.27 ppm is of four equivalent *N*-Me groups, a singlet at δ 6.40 ppm corresponds to benzylic CH proton and a multiplet at δ 7.24–7.44 ppm to the phenyl ring. Two broad singlets at δ 9.62 and 16.2 ppm correspond to the NH group of triethylammonium salt moiety and eight-membered intramolecular H-bonding, respectively (this extra deshielded proton is denoted by H_bg in Fig. 1a and by H_b in Scheme 5b).

The ^{1}H NMR spectra of Michael adducts containing *o*-nitro substituted phenyl ring (**4ab′** and **4ae′**) show an extremely low field for intramolecular H-bonded proton. In particular, in ^{1}H NMR spectroscopy, the proton is increasingly deshielded with increasing hydrogen bond strength, which leads to ^{1}H downfield shifts that are correlated with the length of the hydrogen bond [37–39]. Thus, NMR shift data can be used to estimate lengths of H-bonds [38]. For this reason, we conclude that in compounds **4ab′** and **4ae′**, the donor–acceptor distances ($d_{O\cdots O}$) should be less than 2.50 Å (judging the extremely low field proton chemical shift values at δ 16.25 ppm for H_b in intramolecular eight-membered H-bond in **4ab′** and **4ae′**). For instance, this phenomenon is described for **4ab′** in Scheme 6. Another reported compound consists of delocalized negative charge on barbiturate and the positively charged triethylammonium cation is the triethylammonium 2,4-dinitrophenylbarbiturate [40].

We performed NMR examinations on the bis-barbiturate of **4ae′** derived from the reaction of unsymmetric barbituric acid as 1-MBA (**2e′**) with **1a**. The ^{1}H NMR spectrum of this compound shows a triplet at δ 1.15 and a quartet at δ 3.09 ppm corresponding to methyl and methylene groups of triethylammonium salt moiety, a singlet at δ 3.03 ppm is of two equivalent *N*-Me groups, a singlet at δ 6.18 ppm

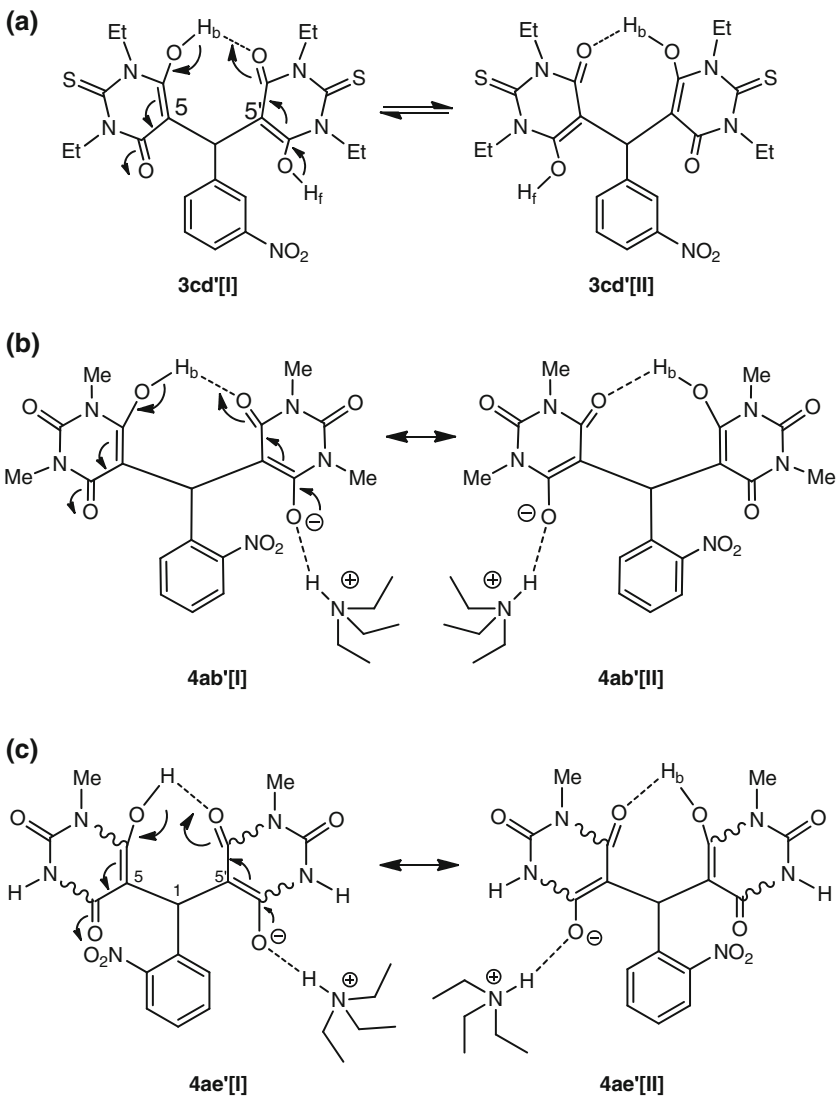

Scheme 5 Tautomeric and mesomeric forms and intramolecular H-bond in **3cd′** (**a**), **4ab′** (**b**) and **4ae′** (**c**). H_b: H-bonding, H_f: H-free)

corresponds to benzylic CH proton and a multiplet at δ 7.23–7.42 ppm to phenyl ring. A broad singlet at δ 8.80, a singlet at δ 10.28 and a broad singlet at δ 16.25 ppm correspond to the NH group of triethylammonium salt moiety, two equivalent NH groups of bis-barbiturate moiety and eight-membered intramolecular H-bonding, respectively (Fig. 1b; Scheme 5c). The ^{1}H NMR data derived from **4ae′** indicated that the bis-barbiturate moiety in this compound has symmetric structure and a fast intramolecular mesomerization occurred. Two mesomeric forms, **4ae′[I]** and **4ae′[II],** do not have a long time on the NMR timescale. Therefore, two methyl and NH groups on geminal bis-barbiturate have chemical shift equivalent (Fig. 1b; Scheme 5c). Similar to **4ab′** as mentioned above, the negative charge is delocalized in the bis-barbiturate moiety of **4ae′**.

Previously, Jursic et al. [25–27] and Neumann et al. [23] have reported the zwitterionic form of pyridinium and quinolinium bis-barbiturates, respectively. The various ammonium salts of some bis-barbiturates have also been reported by the same authors groups [23]. In these compounds, the intramolecular H-bonded proton appeared as hydride bridge and this proton is not detected in their ^{1}H NMR spectra [25–27]. In contrast, in our current research, the intramolecular H-bonded proton (H_b) in triethylammonium bis-barbiturates derived from **2b′** and **2e′** (**4ab′** and **4ae′**, respectively) were detected by ^{1}H NMR spectroscopy and appeared in the ultra deshielded field (at δ 16.25 ppm). This proton is delocalized between two oxygen atoms of O5 and O7 (O5···H_b···O7). Instead, the negative charge delocalized and was able to resonate between the two terminal oxygen atoms of O4 and O6 in the bis-barbiturate moiety as shown in Scheme 6.

It is apparent that the strengthening of the homonuclear O–H···O bond is paralleled by a transition from dissymmetric to symmetric properties of the X1–O–H···O–X2

Scheme 6 Delocalization of negative charge in **4ab′**

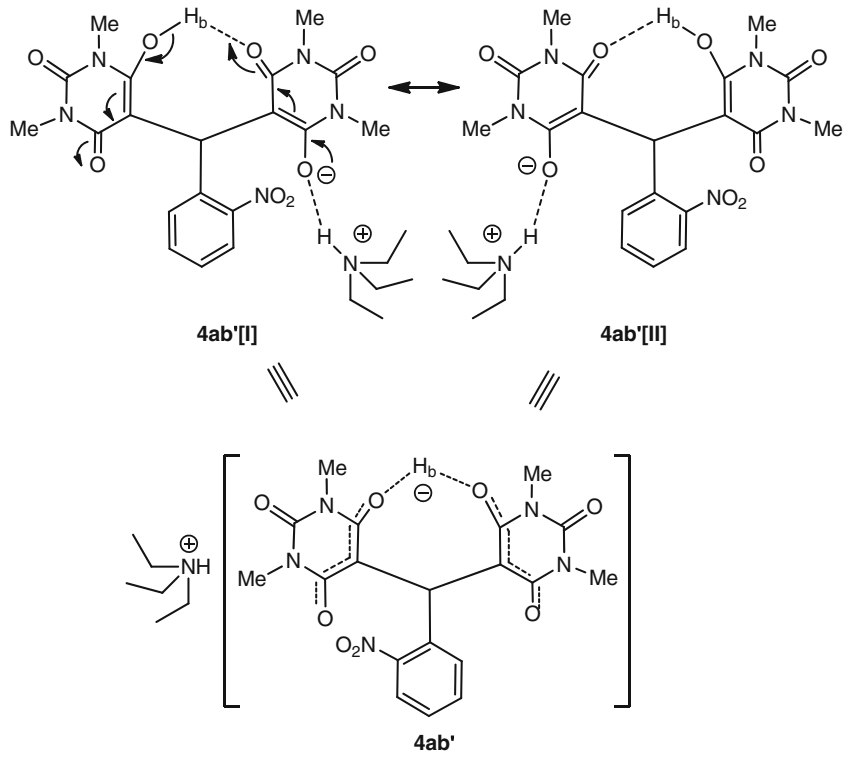

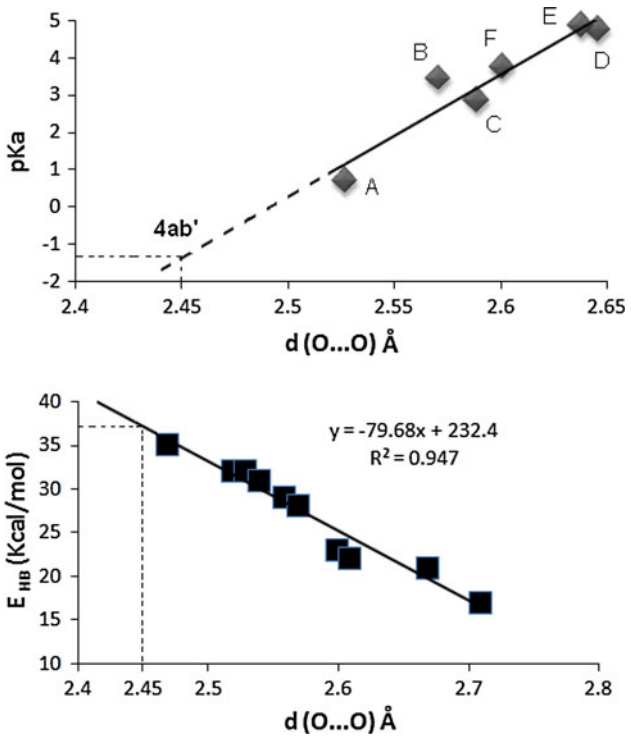

Fig. 2 Correlation of *d*(O5···O7) distance (2.45 Å) in **4ab′** with increasing p*K*a values of trichloroacetic (*A*), chloroacetic (*B*), 2,6-dimethoxybenzoic (*C*), propionic (*D*), acetic (*E*) and formic acids (*F*) [42–45] and estimation of the p*K*a value for **4ab′** (*top*). Hydrogen bond strength (E_{HB}) versus *d*(O5···O7) distance (*bottom*) [46]. Estimation of the p*K*a and E_{HB} (kcal/mol) values for intramolecular H-bond of **4ab′** (···)

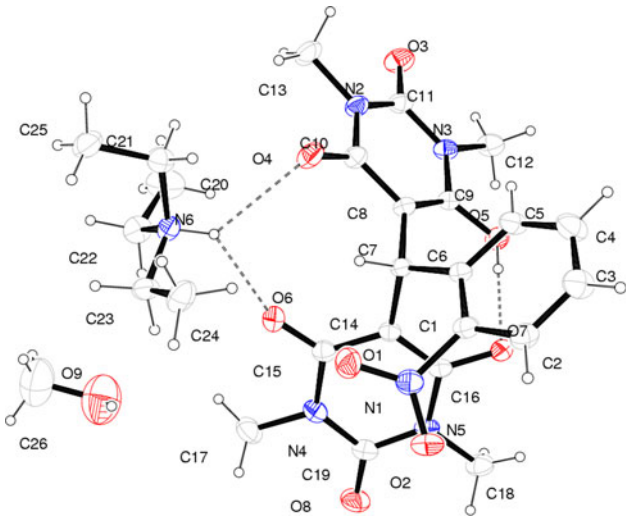

Fig. 3 ORTEP diagram of the molecule **4ab′**. Thermal ellipsoids are shown at the 50 % probability level. *Dashed lines* indicate H-bonding geometry

fragment involved, the condition X1 = X2 included. Very strong H-bonds are essentially three-center four-electron covalent bonds. The strongest H-bonds are homonuclear (X–H···X) and symmetrical as far as the distribution of chemical groups on the two sides of the H-bond is concerned, because only in this situation the two valence bond (VB) resonance forms X–H···X↔X···H–X are isoenergetic and can mix at the greatest extent [21]. Therefore, in this

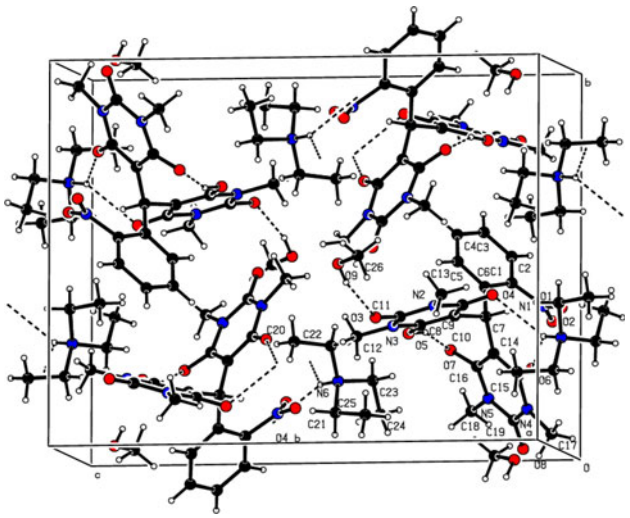

Fig. 4 Unit cell and the H-bonding geometry of the structure of **4ab′**

Table 1 Intra- and intermolecular H-bond length and angles of **4ab′**

D–H···A	*d*(D–H)	*d*(H···A)	*d*(D···A)	<(DHA)	Directionality
O5–H5···O7	0.82	1.70	2.450(5)	152	Strong
N6–H6···O6	0.91	2.20	2.895(5)	133	Moderate
N6–H6···O4	0.91	2.46	3.138(6)	131	Weak
O9–H9···O3	0.82	2.08	2.869(8)	162	Moderate

research, the type of intramolecular H-bonding can be formed as negative charge-assisted H-bonds [(−)CAHB] and resonance-assisted H-bonds (RAHB). Based on bar chart of *d*(O···O) distances (*d*, Å) in organic compounds, subdivided into H-bond strength subclasses, $2.40 \leq d(\mathrm{O{\cdot}O}) \leq 2.50$ and $2.46 \leq d(\mathrm{O{\cdots}O}) \leq 2.65$ Å are attributed to (−)CAHB and RAHB, respectively, and are of strong H-bonds [21]. The intramolecular H-bonds in **4ab′** and **4ae′** are classified as strong, judging from the intramolecular *d*(O5···O7) distance of 2.450 Å for **4ab′** and are of homonuclear O–H···O bond. Instead, the intermolecular H-bond of Et_3N^+6–H6···$^-$O6–C15 is typically heteronuclear and can be classified as positive/negative charge-assisted H-bonds [(±)CAHBs]. The $d(N^+6\cdots{}^-O6)$ and $d(N^+6\cdots{}^-O4)$ distances were obtained as 2.895 and 3.138 Å, respectively. These bonds are usually indicated as "salt bridges" in the biochemical literature and are not only found in proteins, but also in supramolecular chemistry [37, 41].

Comparison of the strength of the H-bond in **4ab′** with other carboxylic acids and flavone-acid compounds reported by Wallet et al. [42–44] and methyl 2,4-dimethoxysalicilate by Dabbagh et al. [45] allows for estimation of the p*K*a of the bis-barbiturates as **4ab′**. They used this method when the experimental p*K*a determination was impractical.

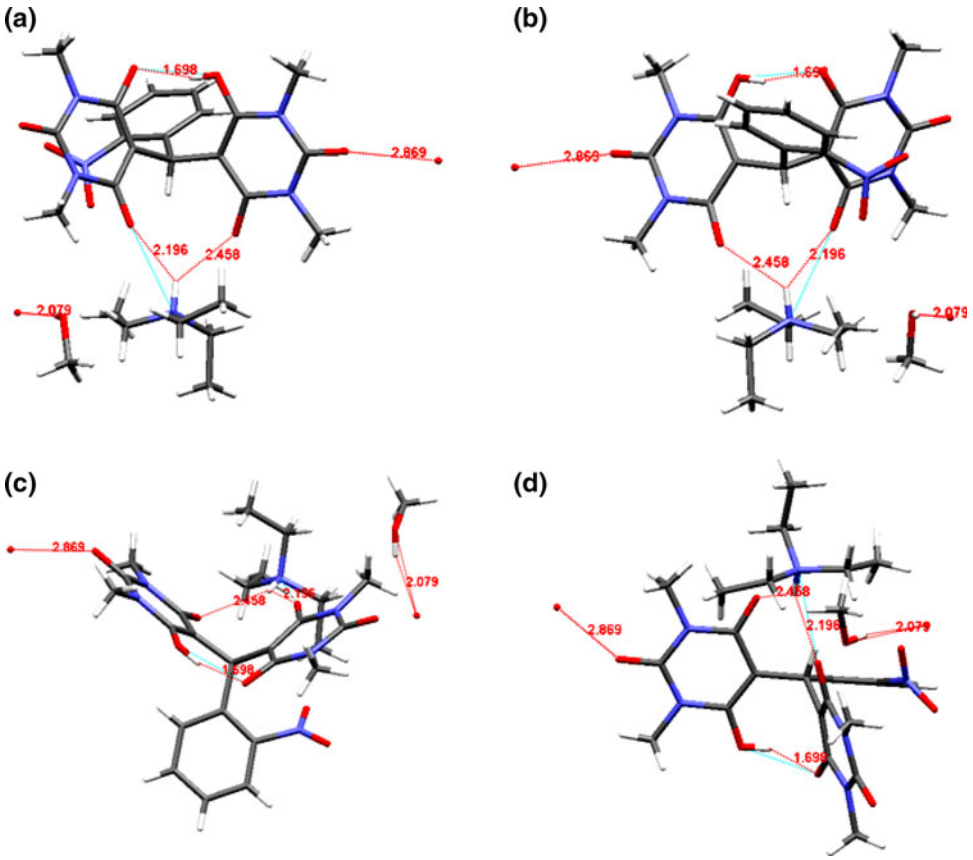

Fig. 5 Inter- and eight-membered intramolecular H-bonds and their distances (Å) in **4ab′**. Views from back (**a**); front (**b**); top (**c**) and bottom side of *o*-nitro phenyl substituent (**d**)

Table 2 Selected crystallographic data of **4ab′**

Empirical formula	$C_{19}H_{18}N_5O_8 \cdot C_6H_{16}N \cdot CH_4O$
Crystal color	Yellow
Fw	578.62
Crystal system	Monoclinic
Space group	$P2_1/n$
Crystal size (mm^3)	0.3 × 0.2 × 0.1
Z	4
a (Å)	10.4938 (2)
b (Å)	14.3340 (4)
c (Å)	18.6166 (4)
a (°)	90.0
β (°)	94.503 (12)
γ (°)	90.0
V ($Å^3$)	2791.63 (11)
ρ_{calcd} (g cm^{-3})	1.38
μ (mm^{-1})	0.105
$F(000)$	1232
θ range (deg)	2.2–26.5
Limiting indices	$-13 \le h \le 13$
	$-16 \le k \le 17$
	$-23 \le l \le 23$
Measured reflections	58850
Independent reflections	5727 [$R_{int} = 0.1184$]
Goodness of fit on F^2	1.016
Final R indices [$F^2 > 2\sigma(F^2)$]	$R1 = 0.088$, w$R2 = 0.169$
Data/restrains/parameters	3826/0/377
Extinction coefficient	0.0
Largest diff. peak and hole ($Å^{-3}$)	0.349 and −0.375

Table 3 Selected bond lengths (Å), angles (θ, °) and torsion angles (φ, °) for **4ab′**

Atom	Bond length (Å), angles (θ, °) and torsion angles (φ, °)
O5–H5A	0.8200
O6–C15	1.236 (5)
O4–C10	1.239 (5)
N6–H6	0.9100
C7–C6	1.534 (6)
C7–H7	0.9800
C9–O5–H5A	109.5
C8–C7–C14	114.7 (3)
C8–C7–H7	104.5
C14–C7–H7	104.5
C6–C7–H7	104.5
C21–N6–H6	106.2
C8–C7–C6–C5	−1.0 (6)
C8–C7–C6–C1	178.0 (4)
C14–C7–C6–C1	−48.5 (5)
C8–C7–C14–C16	88.1 (5)
O1–N1–C1–C2	123.3 (5)

The estimated pKa value for intramolecular H-bond of **4ab′** is equal to ∼−1.3 (Fig. 2, top). Based on correlation between hydrogen bond strength (E_{HB}) and d(O···O) distance, [46], the estimated E_{HB} of intramolecular H-bond for **4ab′** is ∼37 kcal/mol (Fig. 2, bottom).

X-Ray analysis of compound 4ab′

For further study, an X-ray diffraction analysis of **4ab′** was undertaken. The results of this study confirmed unambiguously the crystal structure of **4ab′** (Fig. 3). The crystal packing diagram of **4ab′** is shown in Fig. 4. Triethylammonium salt moiety and a methanol molecule are banded to the bis-barbiturate anion. Intermolecular bifurcated H-bond was also formed between Et_3N^+6–H6···$^-$O6–C15 (N6–H6···O6) and Et_3N^+6–H6···$^-$O4–C10 (N6–H6···O4) atoms in the molecule. The H-bond distance between H6···O6 is found to be little shorter than that of H6···O4 ($\Delta d = 0.26$ Å). The N6–H6···O6 hydrogen bond between the asymmetric units is the main driving force for the orientation of the triethylammonium cation. Other compounds consisting of bifurcated inter- and intramolecular H-bonds have also been reported [38, 47, 48].

An eight-membered intramolecular H-bond was also formed between O5–H5A···O7 atoms. The inter- and intramolecular H-bond distances were found in results of 2.895(5) and 2.450(5) Å, respectively. The corresponding inter- and intramolecular H-bond angles of N6–H6···O6 and O5–H5A···O7 were 133 and 152°, respectively (Table 1). The methanol molecule has an intermolecular H-bonding with O3 atom of the carbonyl group on the bis-barbiturate moiety (Fig. 4). The H-bond length and d(O9···O3) distance were found to be 2.08 and 2.869(8) Å, respectively (Table 1). The crystal structure of **4ab′** is shown from different views of *o*-nitro phenyl substituent in Fig. 5.

A single yellow crystal of **4ab′** was obtained by slow evaporation from methanol at room temperature. For the crystal structure determination, the single crystal of the compound **4ab′** was used for data collection on a four-circle Rigaku R-AXIS RAPID-S diffractometer (equipped with a two-dimensional area IP detector). The graphite-monochromatized MoK_α radiation ($\lambda = 0.71073$ Å) and oscillation scan technique with $\Delta\omega = 5^\circ$ for one image was used for data collection. The lattice parameters were determined by the least-squares methods on the basis of all reflections with $F^2 > 2\sigma(F^2)$. Integration of the intensities, correction for Lorentz and polarization effects and cell refinement were performed using CrystalClear (Rigaku/MSC Inc., 2005) software [49]. The structures were solved

by direct methods using SHELXS-97 [50] and refined by a full-matrix least-squares procedure using the program SHELXL-97 [50]. The crystallographic data and selected bond lengths, angles and torsion angles are summarized in Tables 2 and 3, respectively. Crystallographic data were deposited at CCDC Registration Number 846864 and are available free of charge upon request to CCDC, 12 Union Road, Cambridge, UK (Fax: +44-1223-336033, e-mail: deposit@ccdc.cam.ac.uk).

Acknowledgments We gratefully acknowledge the financial support by the Research Council of Urmia University.

References

1. M. Nishio, Tetrahedron **61**, 6923–6950 (2005)
2. X.-B. Wang, H. K Woo, B. Kira, L.-S. Wang. Angew. Chem. Int. Ed. **44**, 4968–4972 (2005)
3. R.M. McKinlay, P.K. Thallapally, G.W.V. Cave, J.L. Atwood, Angew. Chem. Int. Ed. **44**, 5733–5736 (2005)
4. H. Gong, M.J. Krische, J. Am. Chem. Soc. **127**, 1719–1725 (2005)
5. A. Tessa ten Cate, P.Y.W. Dankers, R.P. Sijbesma, E.W. Meijer, J. Org. Chem. **70**, 5799-5803 (2005)
6. P. Prabhakaran, V.G. Puranik, G.J. Sanjayan, J. Org. Chem. **70**, 10067–10072 (2005)
7. I. Azumaya, D. Uchida, T. Kato, A. Yokoyama, A. Tanatani, H. Takayanagi, T. Yokozawa, Angew. Chem. Int. Ed. **43**, 1360–1363 (2004)
8. Y. Zhu, D.G. Drueckhammer, J. Org. Chem. **70**, 7755–7760 (2005)
9. C.P. Price, A.J. Matzger, J. Org. Chem. **70**, 1–6 (2005)
10. X. Zhang, H. Du, Z. Wang, Y.-D. Wu, K. Ding, J. Org. Chem. **71**, 2862–2869 (2006)
11. I. Alfonso, M.I. Burguete, S.V. Luis, J. Org. Chem. **71**, 2242–2250 (2006)
12. M.H. Abraham, R.J. Abraham, J. Byrne, L. Griffiths. J. Org. Chem. **71**, 3389–3394 (2006)
13. G.A. Jeffery, W. Saenger, *Hydrogen bonding in biological structures* (Springer-Verlag, Berlin, Germany, 1991)
14. A.M. Asiri, S.A. Khan, S.W. Ng, Acta Cryst. Sect. E. **65**, o1860–o1861 (2009)
15. Y. Zhang, C.-S. Wang, J. Comput. Chem. **30**, 1251–1260 (2009)
16. Y.-D. Wu, K.W.K. Chan, D.-P. Wang, J. Am. Chem. Soc. **118**, 9794–9795 (1996)
17. D. Yang, J. Qu, B. Li, F.-F. Ng, X.-C. Wang, K.-K. Cheung, D.-P. Wang, Y.-D. Wu, J. Am. Chem. Soc. **121**, 589–590 (1999)
18. A. G. J. Ligtenbarg, R. Hage, A. Meetsma, B. L. Feringa, J. Chem. Soc., Perkin Trans. **2**, 807–812 (1999)
19. C. Peter, X. Daura, W.F. van Gunsteren, J. Am. Chem. Soc. **122**, 7461–7466 (2000)
20. N. Noroozi Pesyan, M. Jalilzadeh, Turk. J. Chem. **36**, 788–804 (2012)
21. G. Gilli, P. Gilli, J. Mol. Struct. **552**, 1–15 (2000)
22. P. Gilli, V. Bertolasi, L. Pretto, V. Ferretti, G. Gilli, J. Am. Chem. Soc. **126**, 3845–3855 (2004)
23. D. Neumann, "*The Design and Synthesis of Novel Barbiturates of Pharmaceutical Interest*". University of New Orleans Theses and Dissertations. Paper 1040 (2004) http://scholarworks.uno.edu/td
24. A.I. Vogel, A.R. Tatchell, B.S. Furnis, A.J. Hannaford, P.W.G. Smith, *Vogel's textbook of practical organic chemistry*, 5th edn. (Longman, UK, 1989)
25. B.S. Jursic, D.M. Neumann, K.L. Martin, E.D. Stevens, Org. Lett. **4**, 811–813 (2002)
26. B.S. Jursic, D.M. Neumann, Z. Moore, E.D. Stevens, J. Org. Chem. **67**, 2372–2374 (2002)
27. B.S. Jursic, J. Heterocycl. Chem. **40**, 167–170 (2003)
28. J. Adamson, B.J. Coe, H.L. Grassam, J.C. Jeffery, S.J. Coles, M.B. Hursthouse, J. Chem. Soc. Perkin Trans. **1**, 2483–2488 (1999)
29. M. Jalilzadeh, N. Noroozi Pesyan, F. Rezaee, S. Rastgar, Y. Hosseini, E. Şahin, Mol. Divers. **15**, 721–731 (2011)
30. M. Jalilzadeh, N. Noroozi Pesyan, Bull. Korean Chem. Soc. **32**, 3382–3388 (2011)
31. M. Jalilzadeh, N. Noroozi Pesyan, J. Korean Chem. Soc. **55**, 940–951 (2011)
32. N. Noroozi Pesyan, M. Jalilzadeh, J. Chem. Sci. Tech. (JCST) **1**, 1–8 (2012)
33. N. Noroozi Pesyan, S. Rastgar, Y. Hosseini, Acta Cryst. Sect E. **65**, o1444 (2009)
34. Y. Hosseini, S. Rastgar, Z. Heren, O. Büyükgüngör, N. Noroozi Pesyan, J. Chin. Chem. Soc. **58**, 309–318 (2011)
35. M.N. Elinson, A.N. Vereshchagin, N.O. Stepanov, P.A. Belyakov, G.I. Nikishin, Tetrahedron Lett. **51**, 6598–6601 (2010)
36. R.L. Schriner, R.C. Fusan, D.Y. Curtin, T.C. Morrill, *The systematic identification of organic compounds*, 6th edn. (Wiley, New York, 1980)
37. G. A. Jeffrey, *An Introduction to Hydrogen Bonding* (Oxford University Press, Oxford, 1997)
38. T. Steiner, Angew. Chem. Int. Ed. **41**, 48–76 (2002)
39. T.K. Harris, Q. Zhao, A.S. Mildvan, J. Mol. Struct. **552**, 97–109 (2000)
40. D. Kalaivani, R. Malarvizhi, Acta Cryst. Sect. E. **65**, o2548 (2009)
41. E.V. Anslyn, D.A. Dougherty, *Modern Physical Organic Chemistry*. Sausalito, CA: University Science Books, ISBN 1-891389-31-9 (2006)
42. J.-C. Wallet, E. Molins, C. Miravitlles, J. Phys. Org. Chem. **11**, 751–755 (1998)
43. J.C. Wallet, E. Molins, C. Miravitlles, Struct. Chem. **11**, 319–323 (2000)
44. E. Espinosa, E. Molins, J.-C. Wallet, J. Phys. Org. Chem. **12**, 499–502 (1999)
45. H.A. Dabbagh, N. Noroozi Pesyan, B.O. Patrick, B.R. James, Can. J. Chem. **82**, 1179–1185 (2004)
46. J. Chen, M.A. McAllister, J.K. Lee, K.N. Houk, J. Org. Chem. **63**, 4611–4619 (1998)
47. N. Noroozi Pesyan, Magn. Reson. Chem. **47**, 953–958 (2009)
48. P. Gregory, Dyes Pigment. **7**, 45–56 (1986)
49. Rigaku/MSC, Inc., 9009 new Trails Drive, The Woodlands, TX 77381
50. G.M. Sheldrick, *SHELXS97 and SHELXL97* (University of Göttingen, Germany, 1997)